

Negative effective permeability at optical frequencies produced by rings of plasmonic dimers

D. K. Morits and C. R. Simovski

*Department of Radio Science and Engineering, School of Science and Technology, Aalto University,
P.O. Box 13000, FI-00076 AALTO, Finland*

(Received 27 January 2010; revised manuscript received 28 April 2010; published 17 May 2010)

In this paper a design solution for creating the artificial magnetic response of nanostructured metamaterials in the optical frequency range is suggested. This design solution is a modification of the known effective rings formed by plasmonic nanospheres (located at the corners of a regular polygon). Instead of nanospheres we suggest to use bispheres (dimers) which allow us to provide a stronger robustness to Ohmic absorption in silver and, as a result, obtain the negative permeability at the edge between infrared and visible ranges. The study is presented in view of perspectives for isotropic magnetic and doubly negative metamaterials without strong spatial dispersion in the optical frequency range.

DOI: [10.1103/PhysRevB.81.205112](https://doi.org/10.1103/PhysRevB.81.205112)

PACS number(s): 78.20.Ci, 42.70.Qs, 42.25.Gy, 73.20.Mf

I. INTRODUCTION

In the last several years great efforts have been dedicated toward the development of a novel class of metamaterials with both negative permittivity and permeability [known as double negative (DNG) materials], especially in the optical region. Promising perspectives of such composites inspire researchers to offer new designs and ideas, each having its own advantages and disadvantages. Let us briefly discuss the existing solutions to understand which has a best outlook in this area.

The first approach to achieve DNG materials at optical frequencies is a modification of a well-known design based on metallic split-ring resonators (SRRs) and wires in a host medium.¹ It was experimentally shown¹ that this design really leads to DNG material in the microwave regime. However, scaling down SRRs to the optics meets certain difficulties, especially because due to the material properties of metals in optics the permeability tends to approach to the permeability of free space.

The next, not so evident, minus of such structures is that not all of them can be described only in terms of ϵ and μ . Such structures like dual nanobars and nanorods,²⁻⁵ U-shaped SRRs,⁶⁻⁸ and others are not free of high-order multipole response accompanying the magnetic response. Such media called multipolar media or media with weak spatial dispersion were discussed in Refs. 9 and 10. Correct material equations for multipole media contain beside macroscopic fields \mathbf{E} and \mathbf{H} also spatial derivatives of \mathbf{E} .^{9,10} Respectively, more material parameters are needed. The same problem refers to a structure made of pairs of silver spheres, which also have an inevitable quadrupole moment, that is the same order as a magnetic moment and also cannot be described as purely magnetic dipoles as shown in Ref. 11.

The next interesting design for DNG materials is optical fishnet structures (see, e.g., in Refs. 12–15). It has been experimentally demonstrated that ϵ and μ retrieved from the reflection and transmission coefficients of a layer of such structure for the normal incidence reach negative values. However, it is still questionable, how these parameters can be suitable to solve real boundary problems. The reason for this doubt is the geometry of fishnets. They have optically

large periods in the plane parallel to the interface and rather small separation between layers. Therefore fishnets can be homogenized in an only case when the propagation occurs in the normal direction. For obliquely propagating waves multilayer fishnets are lossy photonic crystals and a single-layer fishnet is a lossy electromagnetic band-gap surface. It means that obtained ϵ and μ are only suitable to solve the problem of the normal incidence, which is already solved, because the reflection and transmission coefficients must have been known previously to retrieve ϵ and μ .

Our interests are related with so-called local magnetic permeability¹⁶ which would give a condensed description of magnetic properties of the composite medium, i.e., would be applicable to solve boundary problems and would have a clear physical meaning. It has to be noticed also that the method of retrieving material parameters of metamaterials from the experimental or simulated plane-wave reflection and transmission coefficients is also a matter of dispute. The most widely applied method today is one suggested in Refs. 17 and 18 as an evolution of classical method (Nicholson, Ross, and Weir) of characterization of continuous media (see, e.g., in Refs. 19–23). However, rather frequently results obtained using this approach violate causality and passivity principles and the second law of thermodynamics. This contradiction to the fundamental laws of physics cast doubt on the material parameters obtained in such technique. This question was in details considered in overview²⁴⁻²⁷ and in Refs. 24 and 27 the alternative to the classical method was suggested.

In our opinion, the most convincing designs for the artificial magnetism and, as a result, DNG materials in the optical region are, for example, as follows: four-split optical SRRs suggested in Ref. 28, effective nanorings of plasmonic spheres,²⁹ and finally core-shell magnetic clusters.³⁰ Such magnetodielectric media, whose response does not contain resonant quadrupoles and higher multipoles, can be described only by ϵ and μ .

Since the physical mechanism of artificial magnetism is similar in all these designs, we start our paper from a detailed discussion of the design solution suggested in Ref. 29. The minimal allowed number of nanospheres in the effective nanoring is 4. This case is illustrated by Fig. 1. For this design the response to local field \mathbf{H} is the same for wave

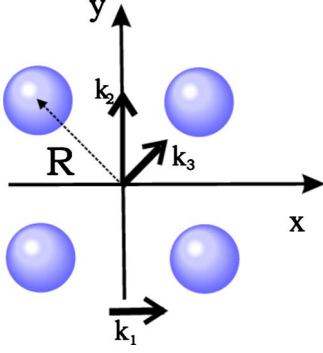


FIG. 1. (Color online) The effective ring of four plasmonic nanospheres is nearly isotropic in the $(x-y)$ plane and a bulk array of such loops can be, in principle, described as a usual magnetodielectric medium.

vectors \mathbf{k}_1 and \mathbf{k}_2 . For wave vector \mathbf{k}_3 the induced magnetic moment will be $\sqrt{2}$ as larger as that for wave vectors $\mathbf{k}_{1,2}$. This obviously means that the effective nanoring of radius R is not fully free of the quadrupole moment. However, a detailed analysis shows that this effect disappears for a composite medium with random arrangement of effective nanorings (unlike random arrays of dual bars and U-SRRs) and the description in terms of only ε and μ is possible.

The objective of the present paper is to modify the known design based on effective rings of plasmonic nanospheres to provide a stronger robustness to Ohmic absorption. We suggest and study the design solution, which allows us to obtain much stronger magnetic resonance than in works^{29,30} and theoretically engineer the negative permeability in the optical range. These goals are achieved by the replacement of simple plasmonic spheres by bispheres (dimers). In the following a transition to an isotropic magnetic nanoclusters potentially leading to isotropic negative permeability at optical frequencies is discussed.

II. EFFECTIVE NANORINGS OF PLASMONIC SPHERES

Let us consider a medium composed by effective nanorings shown in Fig. 1. Nanospheres of radius a are embedded into a host medium with a permittivity ε_h . With notations $k_h = \omega\sqrt{\varepsilon_h\mu_0}$ for background wave number and ε for permittivity of the sphere we can write for its polarizability the well-known formula (see, e.g., in Ref. 29),

$$\alpha = \left[\left(4\pi a^3 \varepsilon_0 \varepsilon_h \frac{\varepsilon - \varepsilon_h}{\varepsilon + 2\varepsilon_h} \right)^{-1} - i \frac{k_h^3}{6\pi \varepsilon_0 \varepsilon_h} \right]^{-1}. \quad (1)$$

The plasmon resonance of the sphere holds at frequency where which $\varepsilon \approx -2\varepsilon_h$. Using the single-dipole approximation for every nanosphere one can express the magnetic polarizability β of the effective ring through Eq. (1) [Eq. (9) from Ref. 29]. A three-dimensional lattice of nanorings forms a composite which effective permeability in the case of optically small lattice period can be estimated using the Maxwell Garnett formula. Following to Ref. 29, we have

$$\mu_{\text{eff}} = \mu_0 \left(1 + \frac{1}{N_d^{-1} [\alpha_{mm}^{-1} + i(k_h^3/6\pi)] - 1/3} \right), \quad (2)$$

where N_d is number of effective rings per unit volume.

We should notice that the effective permeability obtained in this work as well as in the next work¹¹ was calculated with some unlucky considerations that influence quantitative (but not qualitative) results. First of all we need to notice that the permittivity of silver spheres was described in these works by the approximate Drude model which was claimed in Ref. 31 as approximating the experimental data,³²

$$\varepsilon = 5 - \frac{\omega_p^2}{\omega^2 + \omega_d^2} + i \frac{\omega_p \omega}{\omega^2 + \omega_d^2} \quad (3)$$

with plasma frequency $\omega_p/2\pi = 2175$ THz, damping frequency $\omega_d/2\pi = 4.35$ THz, and ultraviolet permittivity $\varepsilon_{UV} = 5$. We compared the original permittivity of silver obtained in Ref. 32 with the Drude model, Eq. (3), and revealed that Eq. (3) is adequate only in the near IR range. If we use it in the visible and near UV ranges we go beyond the limit of its approximation and validity. In more details: at the frequencies less than 400 THz the Drude model gives a really accurate approximation of experimental data but between 400 and 900 THz it describes properly only the real part of permittivity and gives about three times underestimated values for the imaginary part. On the frequencies over 900 THz Drude model cannot be used even for $\text{Re}(\varepsilon)$. The resonant frequencies of nanorings considered in works^{11,29} lie between 450 and 800 THz. Indeed, the error in $\text{Im}(\varepsilon)$ corresponding to Eq. (3) is not fully acceptable for this range. To illustrate this assertion we depict the results for the effective permeability of the composite structure suggested in Ref. 29 using both Drude model, Eq. (3), and experimental data for ε from Ref. 32.

In Fig. 2(a) we see how the magnitude of the resonance of α drops when the evaluative $\text{Im}(\varepsilon)$ is replaced by the experimental one. Respectively, the permeability of effective media after this replacement does not reach negative values in Fig. 2(b). As well we need to notice that the proper attention to the losses is essential in further study of such composites and only experimental data should be used to describe the permittivity of silver in the visible region. We regret to notice that the same Drude model was used in our work³⁰ and the corresponding study shows that the negative permeability is also not reached with substitution of experimental data for $\text{Im}(\varepsilon)$. Thus, to attain negative permeability at optical frequencies we need to use more efficiently polarized structures then plasmonic nanospheres to overcome the reduction of magnetic resonance because of losses in silver.

The next drawback of the model suggested in Ref. 29 already discussed in Ref. 30 is the inadequate homogenization formula (2). It is not applicable if the condition $D \ll \lambda_{\text{eff}}$, where D is the lattice period and λ_{eff} is a wavelength in the host medium is not respected. However, as we checked $D \approx \lambda_{\text{eff}}/2$ at the resonant frequency for all design parameters suggested in works^{11,29} as realizing the negative permeability. Therefore, the quasistatic Maxwell Garnett approxi-

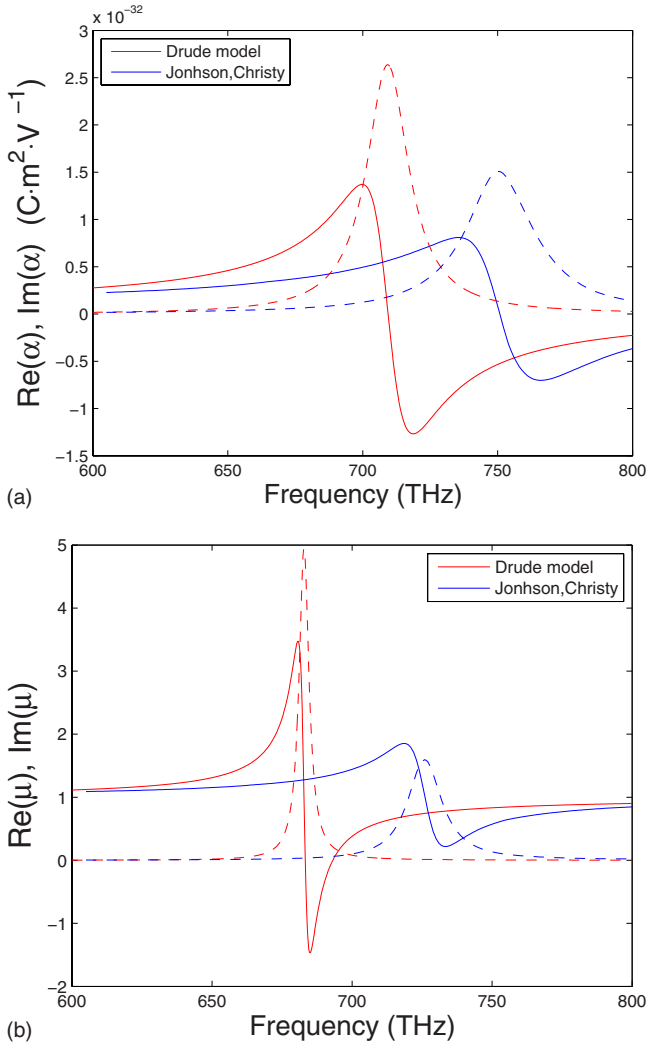


FIG. 2. (Color online) (a) Polarizability of a silver sphere with radius 16 nm (in SI units) both with Drude model and experimental data for the permittivity of silver. Real and imaginary parts of the polarizability are shown by solid and dashed lines, respectively. (b) Effective permeability of the composite media made of rings of silver spheres with radius 16 nm, $R=38$ nm, $N_d=(95 \text{ nm})^{-3}$ both with Drude model and experimental data for the permittivity of silver. Real and imaginary parts of the permeability are shown by solid and dashed lines, respectively.

mation gives only a qualitative estimation of material parameters.

In compliance to the above the main purpose of our work becomes as follows: to modify the effective nanoring so that to provide a stronger robustness to Ohmic absorption in silver and thus obtain the negative effective permeability in the visible or at least in the near IR range using experimental data for ϵ under restriction of rather small optical size of a nanoring [in order to use Eq. (2)]. We will show below that the goal can be achieved by the use of plasmonic dimers.

III. PLASMONIC DIMERS

Studying the literature we found a feasible candidate whose plasmon resonance is much stronger than that of a

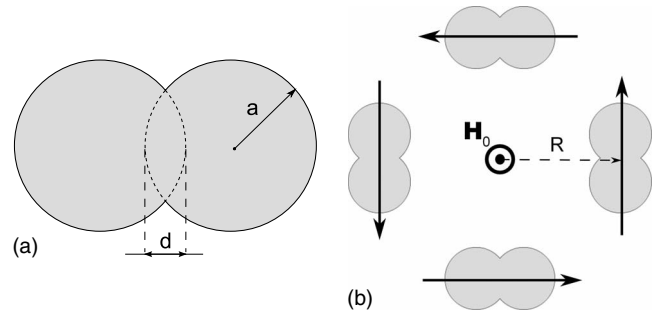


FIG. 3. (a) A plasmonic dimer with spheres of radii a and intersection parameter d . (b) The effective ring made of plasmonic dimers is excited by high-frequency magnetic field H_0 directed orthogonally to its plane. The induced electrical dipole moments are shown by black arrows.

plasmonic nanosphere. It is a plasmonic dimer, i.e., an intersecting pair of spheres shown in Fig. 3(a). The polarizability of a silver dimer has been already studied theoretically in works^{33,34} and experimentally in Ref. 35. In the work³⁴ the problem was solved in a static approximation and the solution in the form of an apparently converging series was based on the Laplace equation written in toroidal coordinate system. Our study of the solution has shown that this solution is applicable for $k_p a < 1$ for dimers made of epsilon-positive dielectrics and for plasmonic dimers with very strong intersection $d/a > 1$ (see Fig. 3). Unfortunately, for plasmonic dimers with $d/a < 1$ the series does not converge. The polarizability α_d of a silver dimer was found from a full numerical solutions of Maxwell's equations using the boundary element method in Ref. 33. The strongest plasmon resonance corresponds, namely, to small intersections. In this case the polarizability has several resonances in the optical range which correspond to dipole, quadrupole and higher multipole responses. The magnitudes of the resonances depend on the geometry however the lowest resonance obviously corresponds to the strongest resonance of α_d since it is dipole resonance. At this resonance also the strongly enhanced local field in the crevices between the intersecting spheres was simulated. The increase in the magnitude of the resonance of α_d compared to α leads to the enhancement of the magnetic susceptibility of the nanoring β_d shown in Fig. 3(b) compared to that Fig. 1. The next advantage is that the resonant frequency of dimer is redshifted compared to a single sphere and turns out to be located in the near IR region where the optical losses of silver are significantly smaller than in the visible range. Therefore we get an opportunity to fulfill the objectives claimed above.

As we do not have the analytical expression for the polarizability of the plasmonic dimer we need to use numerical methods for its calculation. In our work we use the finite-element method commercial simulator Ansoft HFSS to obtain the solution for the polarizability of a dimer. To calculate β_d we substitute α_d in formula (9) of Ref. 29. Since we respect the condition $D \ll \lambda$ the effective permeability μ is further obtained from Eq. (2).

IV. NANORINGS OF PLASMONIC DIMERS

In Figs. 4 and 5 one can see the frequency dependencies of the polarizability of a dimer and the effective permeability

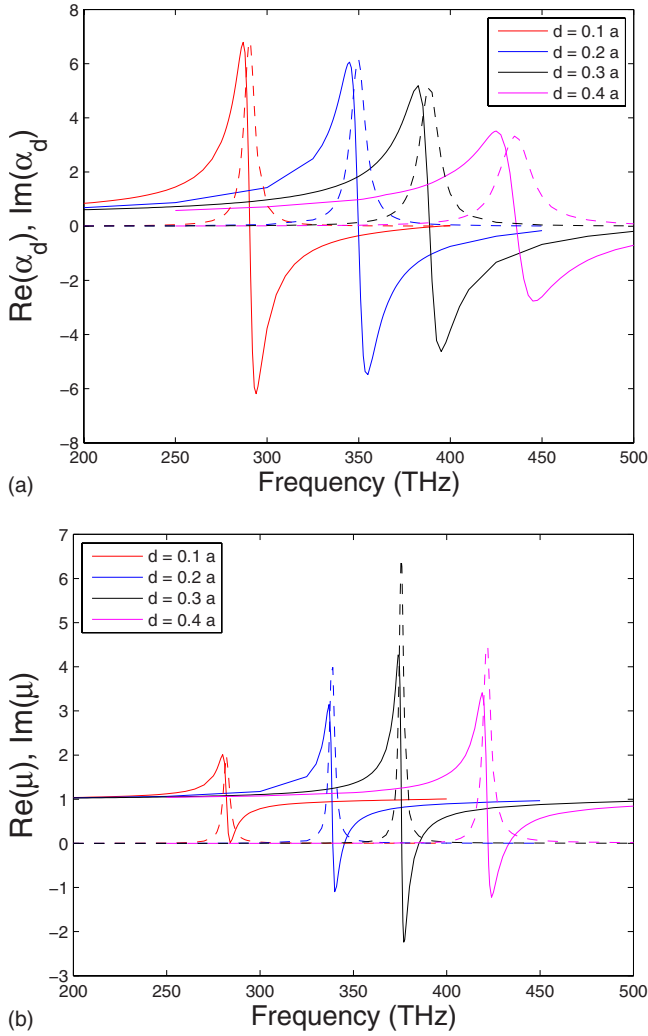


FIG. 4. (Color online) (a) Polarizability of plasmonic dimers with $a=20$ nm for different values of parameter d . Real and imaginary parts of the polarizability are normalized to the same of a single sphere and shown by solid and dashed lines, respectively. (b) Effective permeability of the composite media made of effective rings of four plasmonic dimers with $a=20$ nm, $R=80$ nm, and $N_d=(172 \text{ nm})^{-3}$ for different values of parameter d . Real and imaginary parts of the permeability are shown by solid and dashed lines, respectively.

of composite media in the vicinity of the dipole plasmon resonance. These dependencies are given for different values of the radius of intersecting spheres a and the intersecting parameter d , respectively. The polarizabilities of dimers α_d are normalized to the maximal polarizability of a single sphere $|\alpha_{\text{res}}|$ so that the magnitudes of the resonances could be directly compared.

From Figs. 4 and 5 we can see that our design solution gives us freedom to pick up geometrical parameters of our structure corresponding to the target of negative permeability. For dimers with $a=20$ nm the optimal intersection is $d=0.3a$. For $d=0.2a$, the redshift of the resonant frequency leads to the stronger decrease in optical size of nanoring (see Fig. 4) and the loss in the resonance magnitude can be covered by further increase in a keeping the same optical size at

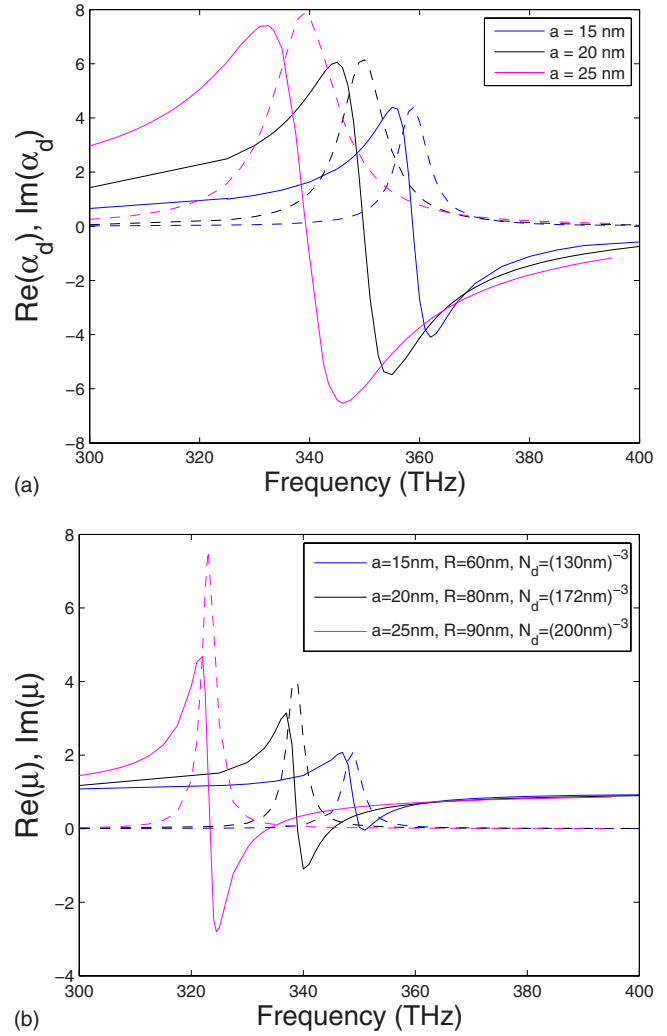


FIG. 5. (Color online) (a) Polarizability of plasmonic dimers with $d/a=0.2$ for different radii of spheres. Real and imaginary parts of the polarizability are normalized to the same of a single sphere and shown by solid and dashed lines, respectively. (b) Effective permeability of the composite media made of rings of plasmonic dimers with $d/a=0.2$ for different radii of spheres. Real and imaginary parts of the permeability are shown by solid and dashed lines, respectively.

the resonance (see Fig. 5). However, the frequency range in which the permeability is negative corresponds to $\lambda=890-930$ nm which is not a so exciting frequency region for us. For $d=0.4a$ the resonance should have been even stronger but so big intersection corresponds to the blueshift and the resonant frequency turns out to be in the visible region where the losses in silver are significantly bigger than in the near IR. Thus, by the proper choice of the intersecting parameter d the resonant frequency can be shifted to region there the optical losses in silver are small enough, the magnetic response is strong enough and which is at the edge between the visible and the IR ranges.

It should be noticed that plasmonic dimers cannot replace plasmonic spheres if we want to obtain the artificial magnetism in the range $f=600-800$ THz since dimers never resonate in this range. However, it is possible to achieve negative

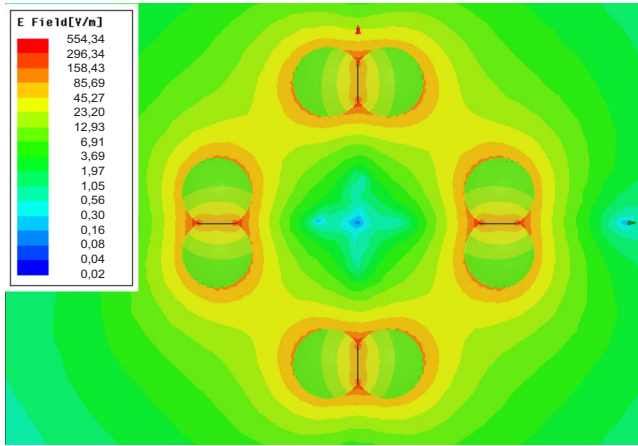


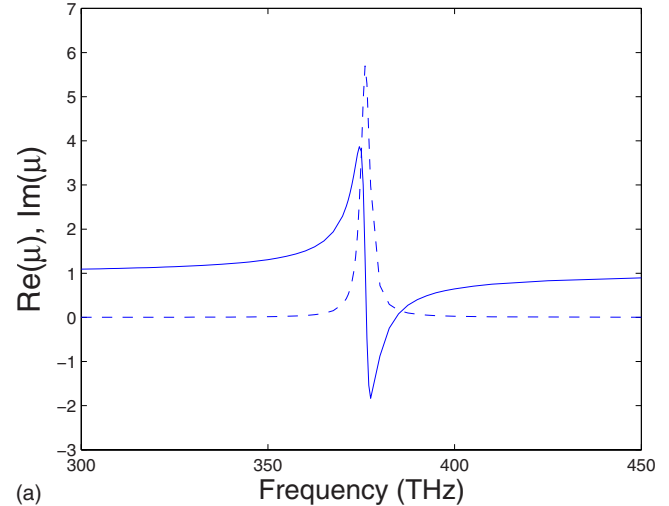
FIG. 6. (Color online) Spatial distribution of the amplitude of electric field at 369 THz for an effective plasmonic loop with $R = 80$ nm comprising four dimers with $a = 20$ nm and $d = 0.3a$. Logarithmic scale.

permeability with dimers at least in the near IR whereas with simple spheres we could not obtain it in both visible and IR ranges. This our result is a demonstration of superiority of plasmonic dimers over plasmonic spheres.

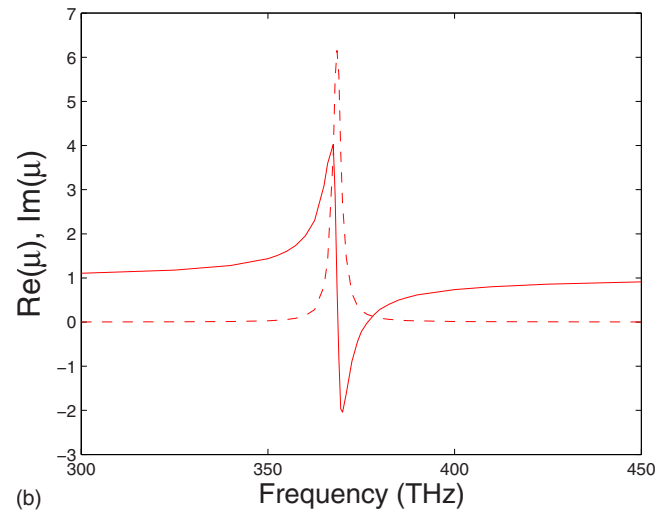
As one can see from the Fig. 5 the increase in the radius of spheres gives us stronger resonance of polarizability of dimer and consequently the stronger magnetic response. At the same time we should remember that the dimensions of our structure are limited as we want to apply a homogenization procedure and describe our medium with material parameters ϵ and μ . For the dimensions shown in Fig. 4 on the resonant frequency, we obtain $D \approx \lambda/5 \approx \lambda_{\text{eff}}/3$, where λ_{eff} is a wavelength in the host medium with $\epsilon_h = 2.2$. This is better than $D \approx \lambda_{\text{eff}}/2$ in the initial design,^{11,29} but we have to admit that the lattice period is not very small, yet, and the quasi-static homogenization model gives only a qualitative estimation of material parameters. It can be improved using the dynamic theory of local material parameters developed in works.^{24,25} This work is planned in the next future.

V. VALIDATION OF THE DIPOLE MODEL OF AN EFFECTIVE NANORING

The theory we used to calculate the magnetic response of the effective nanoring takes into account only dipolar interactions between dimers. Also, the magnetic moment of the nanoring is calculated replacing the dimers by point dipoles. This dipole model is an approximation that should be verified. We have validated our results with full-numerical solutions using a HFSS simulator for a direct calculation of the induced magnetic moment and hence of the magnetic polarizability β . The distribution of the total electric field at the resonant frequency 369 THz for a nanoring with radius $R = 80$ nm prepared of four dimers with $a = 20$ nm and $d = 0.3a$ is shown in Fig. 6. To appreciate the field enhancement in crevices one should note that the amplitude of \mathbf{E} is given in a logarithmic scale. The magnetic moment of the nanoring can be calculated directly using its definition



(a)



(b)

FIG. 7. (Color online) Effective permeability of the composite media made of effective rings of plasmonic dimers with $a = 20$ nm, $d = 0.3a$, $R = 80$ nm, and $N_d = (172 \text{ nm})^{-3}$: (a) theoretical result taking into account only dipolar interactions between particles and (b) results of a full-wave simulation in HFSS. Real and imaginary parts of the permeability are shown by solid and dashed lines, respectively.

$$\mathbf{m} = \frac{1}{2} \int_V \mathbf{J} \times \mathbf{r} dV.$$

Here \mathbf{r} is radius vector referred to the loop center and $\mathbf{J} = i\omega\epsilon_0(\epsilon - \epsilon_h)\mathbf{E}$ is polarization current density inside silver spheres. The local magnetic field \mathbf{H} at the origin corresponds to four incident waves, creating nearly azimuthal polarization of the local electric field around the origin (see in Refs. 11, 29, and 30).

After calculating $\beta = m/H$ we evaluate the effective permeability using the Maxwell Garnett formula. The results of this homogenization are shown in Fig. 7(b) in comparison with previously obtained results of the dipole model presented in Fig. 7(a). The applicability of the dipole model is then confirmed by a good agreement of these results.

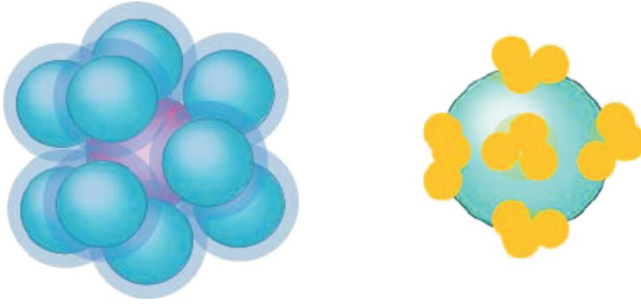


FIG. 8. (Color online) A sketch of a nearly isotropic magnetic scatterers with plasmonic trimers. Left: a metashell of three trimers of plasmonic nanospheres, the core radius is smaller than that of plasmonic nanospheres. Left: a metashell of six plasmonic trimers, the core radius is larger than that of nanospheres.

VI. TOWARD ISOTROPIC OPTICAL MAGNETICS AND ISOTROPIC DOUBLY NEGATIVE MEDIA

As it was noticed above the effective nanoring is not fully isotropic even in its plane. To create an isotropic magnetic composite of such nanorings an array with random orientations of nanoring planes should be prepared. This requirement strongly conflicts with the objective of the negative permeability. In order to obtain the resonance of the permeability strong enough to cross the zero the gaps between adjacent nanorings should be smaller than R . Notice that in papers^{11,29} the suggested density of nanorings was ultimately possible, however it is nearly so also in our case. With the needed concentration to create the random array is practically possible only by price of touching or intersecting adjacent nanorings. Therefore, the results obtained above refer to a regular cubic lattice with period $D=N_d^{(-1/3)}$. This lattice would not be free of quadrupole polarization and is not fully isotropic. To get rid of quadrupole polarization and simultaneously to obtain an isotropic permeability we need to design the isotropic magnetic scatterer.

The transition from a lattice of nanorings toward an isotropic lattice with nearly same negative permeability can be understood from paper.³⁰ Transiting from plasmonic dimers to trimers (tripods) and locating them on the surface of the dielectric core we will obtain the magnetic nanocluster with a practically isotropic plasmonic metashell also experiencing a magnetic resonance in the near IR. Two possible design solutions of nearly isotropic magnetic scatterers based on plasmonic trimers are shown in Fig. 8. It is not clear in

advance which of two suggested design solutions (when the plasmonic nanospheres are larger than the core and when they are smaller) is optimal. Both of them can be manufactured using the self-assembly (see, e.g., in Ref. 30). In our next paper we hope to obtain the similar theoretic results for such isotropic magnetic clusters as those reported in the present paper for effective magnetic loops.

If the isotropic composite medium based on plasmon trimers is realized the next step will be the design of a doubly negative composite. Following to³⁰ this will be probably achievable using the core-shell particle instead of a dielectric core in clusters depicted in Fig. 8. Then the silver or gold core centers the cluster and is surrounded by a dielectric shell to which plasmonic tripods are glued. The central plasmonic nanoparticle of the cluster should help to tune the dipole resonance frequency of the whole cluster so that it would coincide with the magnetodipole resonance of its metashell (as it was obtained in Ref. 30).

VII. CONCLUSION

In the present paper we have discussed the previously obtained theoretical results for structures apparently exhibiting negative effective permeability in the visible and near IR ranges. Our study takes into account experimental results for the permittivity of silver. On the base of the known design of a structure with resonant magnetic response, effective plasmonic loop suggested in Ref. 29, we offered modifications to provide a stronger robustness of the magnetic response to Ohmic loss in silver by replacing plasmonic nanospheres by plasmonic dimers. Our design satisfies the conditions of the optical smallness which is obvious for a homogenization procedure. It theoretically allows us to reach the needed result at the edge between IR and visible ranges. Our theory is partially validated by full-wave simulations. A way of future improvement of this design with the purpose to create a fully isotropic optical composites with negative permeability and with two negative material parameters is outlined. The present paper is the first step in this direction.

ACKNOWLEDGMENTS

The research leading to these results has received funding from the European Community's Seventh Framework Programme (FP7/2007-2013) under grant Agreement No. 228762 and was carried out in the frame of METACHEM project (2009-2013).

¹R. A. Shelby, D. R. Smith, and S. Schultz, *Science* **292**, 77 (2001).

²V. A. Podolskiy, A. K. Sarychev, and V. M. Shalaev, *J. Nonlinear Opt. Phys. Mater.* **11**, 65 (2002).

³A. K. Sarychev and V. M. Shalaev, in *Negative Refraction Metamaterials: Fundamental Properties and Applications*, edited by G. V. Eleftheriades and K. G. Balmain (Wiley, Hoboken, NJ, 2005), Chap. 8, pp. 313–337.

⁴G. Dolling, C. Enkrich, M. Wegener, J. F. Zhou, C. M. Soukoulis, and S. Linden, *Opt. Lett.* **30**, 3198 (2005).

⁵Y. Ekinici, A. Christ, M. Agio, O. J. F. Martin, H. H. Solak, and J. F. Löffler, *Opt. Express* **16**, 13287 (2008).

⁶J. Zhou, Th. Koschny, and C. M. Soukoulis, *Opt. Express* **15**, 17881 (2007).

⁷B. Kanté, A. de Lustrac, J.-M. Lourtioz, and F. Gadot, *Opt. Express* **16**, 6774 (2008).

- ⁸C. Rockstuhl, Th. Zentgraf, E. Pshenay-Severin, J. Petschulat, A. Chipouline, J. Kuhl, Th. Pertsch, H. Giessen, and F. Lederer, *Opt. Express* **15**, 8871 (2007).
- ⁹R. E. Raab and O. L. De Lange, *Multipole Theory in Electromagnetism* (Clarendon Press, Oxford, 2005).
- ¹⁰C. R. Simovski and S. A. Tretyakov, in *Theory and Phenomena of Metamaterials*, Handbook of Metamaterials Vol. 1, edited by F. Capolino (CRC Press, New York, 2009), Chap. 2.
- ¹¹A. Alù and N. Engheta, *Phys. Rev. B* **78**, 085112 (2008).
- ¹²G. Dolling, C. Enkrich, M. Wegener, C. M. Soukoulis, and S. Linden, *Science* **312**, 892 (2006).
- ¹³M. Kafesaki, I. Tsiapa, N. Katsarakis, Th. Koschny, C. M. Soukoulis, and E. N. Economou, *Phys. Rev. B* **75**, 235114 (2007).
- ¹⁴J. Zhou, Th. Koschny, and C. M. Soukoulis, *Opt. Express* **16**, 11147 (2008).
- ¹⁵C. García-Meca, R. Ortuno, F. J. Rodriguez-Fortuno, J. Marti, and A. Martinez, *Opt. Lett.* **34**, 1603 (2009).
- ¹⁶L. D. Landau, L. P. Pitaevski, and E. M. Livshitz, *Electrodynamics of Continuous Media*, 2nd ed. (Elsevier, Burlington, MA, 2004).
- ¹⁷D. R. Smith, S. Schultz, P. Markos, and C. M. Soukoulis, *Phys. Rev. B* **65**, 195104 (2002).
- ¹⁸D. R. Smith, D. C. Vier, T. Koschny, and C. M. Soukoulis, *Phys. Rev. E* **71**, 036617 (2005).
- ¹⁹A. M. Nicolson and G. F. Ross, *IEEE Trans. Instrum. Meas.* **17**, 395 (1968).
- ²⁰W. W. Weir, *Proc. IEEE* **62**, 33 (1974).
- ²¹J. Krupka, *IEEE Trans. Microwave Theory Tech.* **47**, 752 (1999).
- ²²V. N. Egorov, *Instrum. Exp. Tech.* **50**, 143 (2007).
- ²³M. Sucher, *Handbook of Microwave Measurements* (Polytechnic Press, Brooklyn, 1963), Vol. 2.
- ²⁴C. R. Simovski, *Opt. Spectrosc.* **107**, 726 (2009).
- ²⁵C. R. Simovski and S. A. Tretyakov, *Phys. Rev. B* **75**, 195111 (2007).
- ²⁶C. R. Simovski, *Metamaterials* **1**, 62 (2007).
- ²⁷C. R. Simovski, *Metamaterials* **2**, 169 (2008).
- ²⁸J. Zhou, Th. Koschny, M. Kafesaki, E. N. Economou, J. B. Pendry, and C. M. Soukoulis, *Phys. Rev. Lett.* **95**, 223902 (2005).
- ²⁹A. Alù, A. Salandrino, and N. Engheta, *Opt. Express* **14**, 1557 (2006).
- ³⁰C. R. Simovski and S. A. Tretyakov, *Phys. Rev. B* **79**, 045111 (2009).
- ³¹I. El-Kady, M. M. Sigalas, R. Biswas, K. M. Ho, and C. M. Soukoulis, *Phys. Rev. B* **62**, 15299 (2000).
- ³²P. B. Johnson and R. W. Christy, *Phys. Rev. B* **6**, 4370 (1972).
- ³³I. Romero, J. Aizpurua, G. W. Bryant, and F. J. Garcia de Abajo, *Opt. Express* **14**, 9988 (2006).
- ³⁴M. Pitkonen, *J. Math. Phys.* **47**, 102901 (2006).
- ³⁵D. ten Bloemendal, P. Ghenuche, R. Quidant, I. G. Cormack, P. Loza-Alvarez, and G. Badenes, *Plasmonics* **1**, 41 (2006).